PROCEEDINGS OF SPIE

SPIEDigitalLibrary.org/conference-proceedings-of-spie

Laboratory testing and calibration of the upgraded MMT adaptive secondary mirror

Vaz, Amali, Morzinski, Katie, Montoya, Manny, Fellows, Chuck, Ford, John, et al.

Amali Vaz, Katie M. Morzinski, Manny Montoya, Chuck Fellows, John Ford, Andrew Gardner, Olivier Durney, Grant West, Lori Harrison, Frank Gacon, Elwood Downey, Jared Carlson, Emily Mailhot, Narsireddy Anugu, Buell Jannuzi, Phil Hinz, "Laboratory testing and calibration of the upgraded MMT adaptive secondary mirror," Proc. SPIE 11448, Adaptive Optics Systems VII, 114485L (13 December 2020); doi: 10.1117/12.2576352



Event: SPIE Astronomical Telescopes + Instrumentation, 2020, Online Only

Laboratory testing and calibration of the upgraded MMT adaptive secondary mirror

Amali Vaz^a, Katie M. Morzinski^a, Manny Montoya^a, Chuck Fellows^a, John Ford^a, Andrew Gardner^a, Olivier Durney^a, Grant West^a, Lori Harrison^a, Frank Gacon^a, Elwood Downey^a, Jared Carlson^a, Emily Mailhot^a, Narsireddy Anugu^a, Buell Jannuzi^a, and Phil Hinz^b

^aSteward Observatory, University of Arizona, 933 N. Cherry Ave., Tucson AZ 85721, USA ^bCenter for Adaptive Optics, University of California–Santa Cruz, Santa Cruz CA 95064, USA

ABSTRACT

The MMT Adaptive optics exoPlanet characterization System (MAPS) is a broad overhaul and upgrade of AO instrumentation at the 6.5-m MMT observatory, from deformable secondary mirror, through pyramid wavefront sensors in both the visible and near-infrared, to improved science cameras. MAPS is an NSF MSIP-funded program whose ultimate goal is a facility optimized for exoplanet characterization. Here we describe the laboratory testing and calibration of one MAPS component: the refurbished MMT adaptive secondary mirror (ASM). The new ASM includes a complete redesign of electronics and actuators, including simplified hub-level electronics and digital electronics incorporated into the actuators themselves. The redesign reduces total power to <300W, from the original system's 1800W, which in turn allows us to eliminate liquid cooling at the hub with no loss of performance. We present testing strategies, results, and lessons learned from laboratory experience with the MAPS ASM. We discuss calibrations first on the level of individual actuators, including capacitive position sensing, force response function, and individual closed-loop position control with an improved control law. We then describe investigations into the full ASM system – hub, actuators, thin shell, and human – to understand how to optimize interactions between components for dynamical shape control using a feedforward matrix. Finally, we present our results in the form of feedforward matrix and control law parameters that successfully produce a desired mirror surface within 1ms settling time.

Keywords: Adaptive optics, deformable mirrors, adaptive secondary mirrors, feedforward control, MMTAO

1. INTRODUCTION

The MMT AO exoPlanet characterization system (MAPS) is a total overhaul of the AO system at the MMT, with the ultimate goal of creating a facility tailored to the needs of exoplanet characterization science. As part of the MAPS program, we're redesigning, refurbishing, rebuilding, and reintegrating the MMT adaptive secondary mirror (ASM). For an update on the status of the general MAPS project, see (1); for the visible-light wavefront sensor development see (2).

1.1 ASM Improvements

The improvements to the ASM can be classified as follows:

New electronics: Advances in electronics mean we can fit actuator electronics in the body of the actuator itself, and use standard PCs instead of custom-built processors for external computations.

Passive air cooling: Low power means less heat generated at the hub, which in turn means we can do away with complex and leak-prone liquid cooling systems.

Improved control law: The original system ran at 500 Hz. We should be able to reach 1 kHz with the upgraded MAPS ASM.

Further author information: Send correspondence to A.V. at amali@arizona.edu

Adaptive Optics Systems VII, edited by Laura Schreiber, Dirk Schmidt, Elise Vernet, Proc. of SPIE Vol. 11448, 114485L · © 2020 SPIE · CCC code: 0277-786X/20/\$21 · doi: 10.1117/12.2576352

1.2 Performance Requirements

We can claim ASM victory if and only if the following conditions are met:

- \bullet Spatial performance: The ASM can produce a 150-mode surface approximation to a Kolmogorov atmosphere with r_0 of 15 cm at 550 nm.
- Temporal performance: The ASM can settle within 10% of a commanded position within 1 ms after receiving the request.

1.3 ASM Testing and Calibration

Figure 1 shows the components of the ASM that are covered in this work. They are the following parts from the legacy ASM: the central hub, cold plate, reference body, and thin shell. The following parts are completely new builds for the MAPS ASM: 336 new actuators, 6 new daughterboards, 1 new motherboard. In this paper we present the following steps in going from a pile of actuators and electronics to a fully functioning ASM for MAPS: component checkout, calibration, and electrical & optical testing.

2. COMPONENT CHECKOUT

The **motherboard** receives power from the power supply and commands from operators; it produces the master "Go" square wave at 100 kHz; and conveys all of those to the daughterboards. Figure 2 illustrates this checkout.

The six daughterboards direct commands to specific actuator(s) within their sector. This test made use of the individual LEDs on each actuator to test the mapping. Figure 3 illustrates this checkout.

The 336 actuators were tested as follows:

• Report status and information:

- Test: a) report continuous position and current;
- Test: b) report on-demand serial number and configuration parameters.
- Result: 11 actuators report corrupted values. They have been disabled by software and will be investigated.

Acts on operator commands:

- Test: respond to "blink your LED". Also verified raw ethernet packets.
- Result: No additional failed actuators.

• Applies force on command:

- Test: each actuator can suspend a small physical weight when "pull" force is applied.
- Result: No additional failed actuators.

• Reports raw capacitive sensor values:

- Test: a) without shell, produce positive counts when test object is within range.
- Test: b) with shell, report gap at edge consistent with a plastic shim
- Test: c) during operation, report gap < max and ADC counts > 10000
- Result: 10 actuators disabled for reporting 0 ADC counts. 1 actuator disabled for bad armature coating.

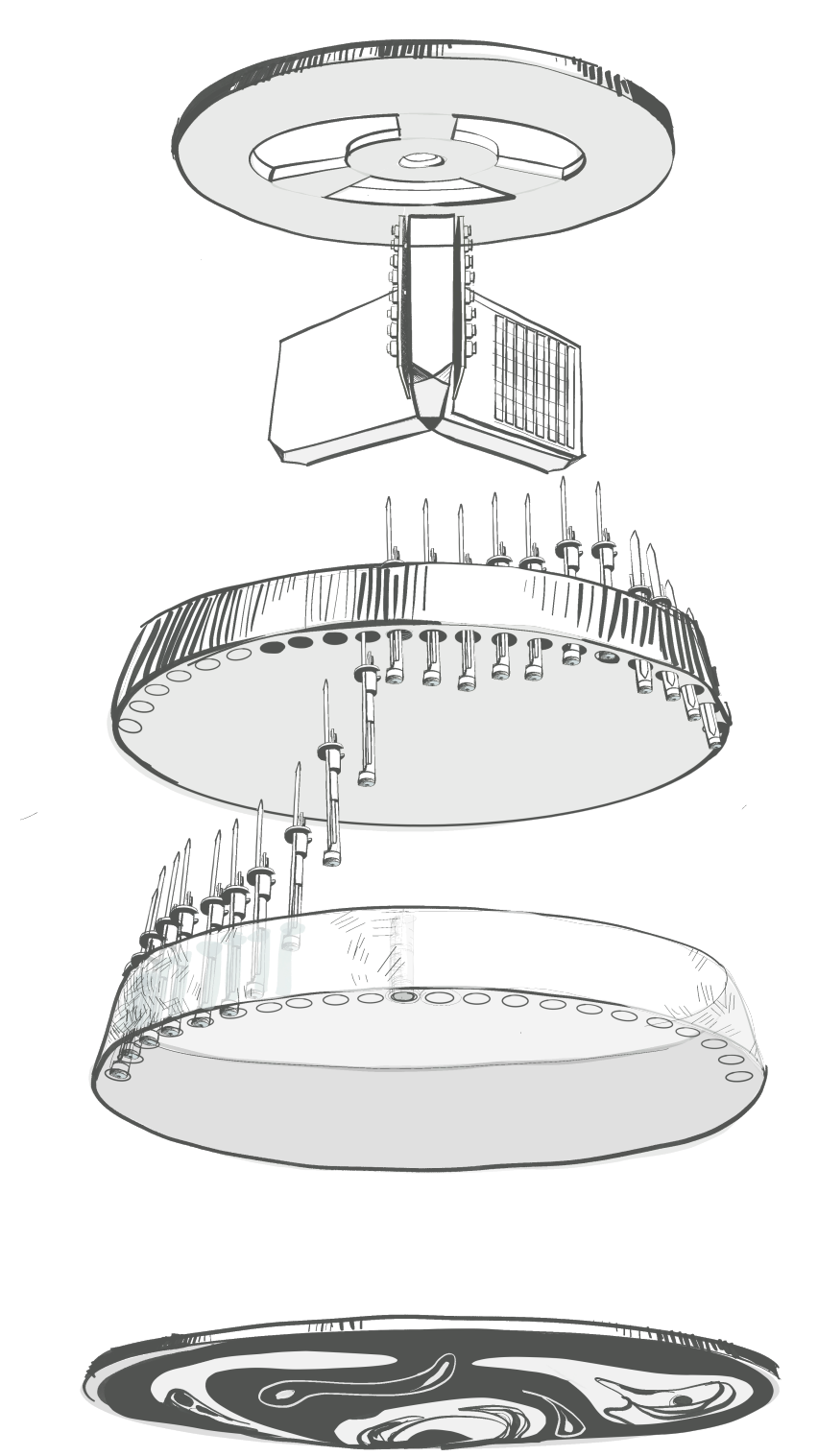


Figure 1 "Exploded" drawing of the adaptive secondary mirror. From top to bottom we have: hub structure (original), 6 daughterboards (new), cold plate (original), reference body (original), and thin shell (original). Inserted in the cold plate and poking through the holes in the reference body are the 336 actuators (new).

Figure 4 illustrates this checkout.





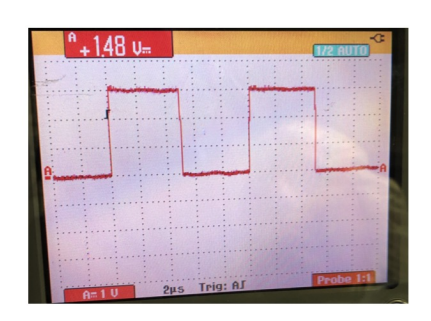


Figure 2 Motherboard checkout. **Left and Center:** Proof of life: actuators are set to blink when powered on. **Right:** "Go" pulse timing and magnitude verified by oscilloscope.

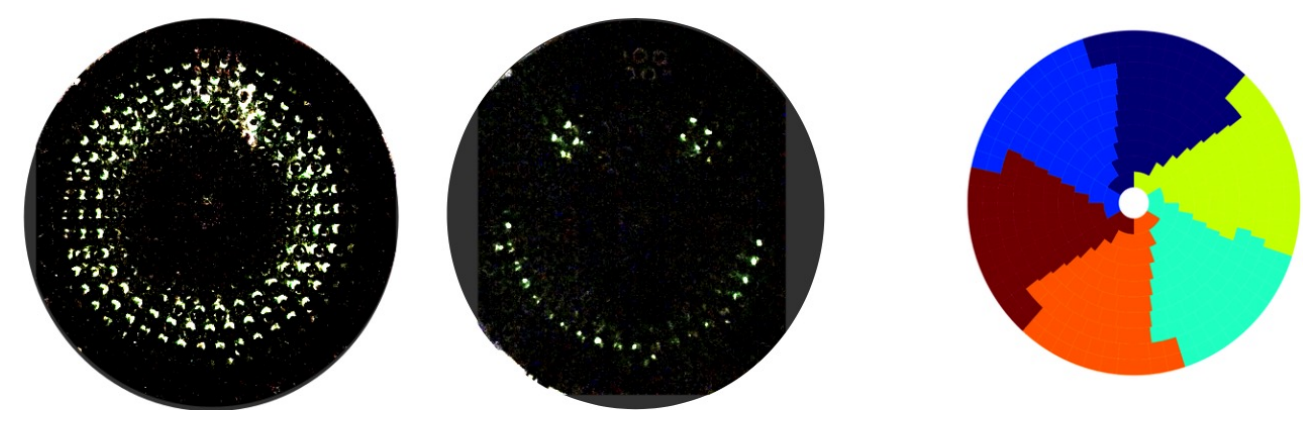


Figure 3 Daughterboard checkout. **Left and Center:** Mapping: we verified that we can control which actuators blink their green LED lights. **Right:** Sector layout of the 6 daughterboards.

Measurement noise. Test: As per the original specification, a 1-second rms of the Measured Position should be <10 nm. Result: All actuators failed! Our rms varies from 15 nm to 35 nm. ~30 actuators were disabled for high rms, bi-stable position readings, or drifting values over time. Meanwhile, we continued with actuators of rms <25 nm. The current "good" list has 281 actuators. Figure 5 illustrates this checkout.

The result of the component testing was a census of 281 actuators enabled overall. Their status is functional, but with open questions regarding the noise.

2.1 Gap

The gap is an all-important cushion of air between the reference body and thin shell. Testing to date has used a nominal value of 35 μ m for the gap; further calibration should allow up to at least 60 μ m. The tradeoff here is between achievable stroke and relaxed contamination standards, on the one hand, and the stability of natural viscous damping on the other.

Tests for contaminants: Apparent topology on a rested shell could be a genuine physical disturbance or simply a miscalibrated capacitive sensor. The hallmark of physical invasion is a "bump" that spreads beyond a single capacitor, and which does not change beyond some threshold coil current pull.

 \sim 30 actuators were installed slightly too low, so that they protruded from the reference body enough to cause a bump on the shell. They were adjusted manually.

The gap was also physically measured with a 25 μ m plastic shim, and was in good agreement with reality. Figure 6 illustrates this checkout.

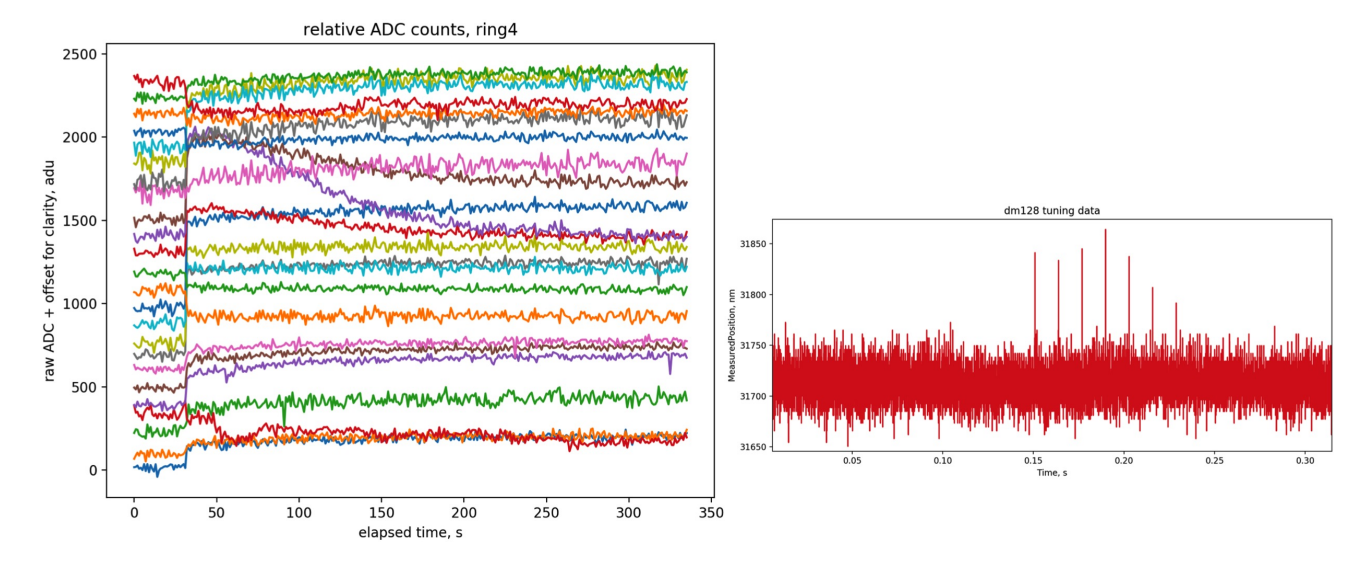


Figure 4 Actuators checkout: an illustration of potentially disqualifying factors in actuator capacitive sensor and position measurement. **Left**: time series of raw capacitive sensor readings (i.e. not converted into position) for the actuators in the 4th concentric ring from the mirror center. At t=40 seconds, the shell was commanded to attain and hold a position. Ideal actuator performance would be a perfectly flat line. Actuators that showed significant systematic deviation -4 of them in this plot - were removed from further calibrations. **Right**: another kind of actuator "noise", possibly caused by electronic interference. This noise doesn't disrupt the overall performance badly enough to remove the actuator.

2.2 Thin Shell

The thin shell is the beneficiary of the actuators' pushing and pulling work. It deforms in response to applied forces.

The gap size is calculated by capacitive sensors on each actuator, but until we correlate electrical and optical measurements, we can't be sure of the reported values. We can, however, use reported values to evaluate any position-dependent effects. Figure 7 illustrates the thin shell tests.

3. CALIBRATION

3.1 Capacitive Sensor Calibration

We monitor thin shell position at each actuator by measuring capacitance between two effectively parallel plates: the upper — a chrome annulus painted on the reference body around each actuator channel (the armatures), and the other — the back surface of the thin shell. We refer to the capacitive sensor as the "cap-sens".

The relationship between cap-sens ADC counts and gap size d is roughly inverse, and characterized by two parameters, Gain and Offset:

$$d = \frac{V * Gain}{ADC + Offset} \tag{1}$$

Applying the system geometry yields a first estimate of calibration. From there, we measure the actual area of chrome around each actuator, because they vary: those in the outermost ring are clipped by design, but many others have significant scrapes or wear (Figure 8).

Figure 9 shows the linear fits and gain results.

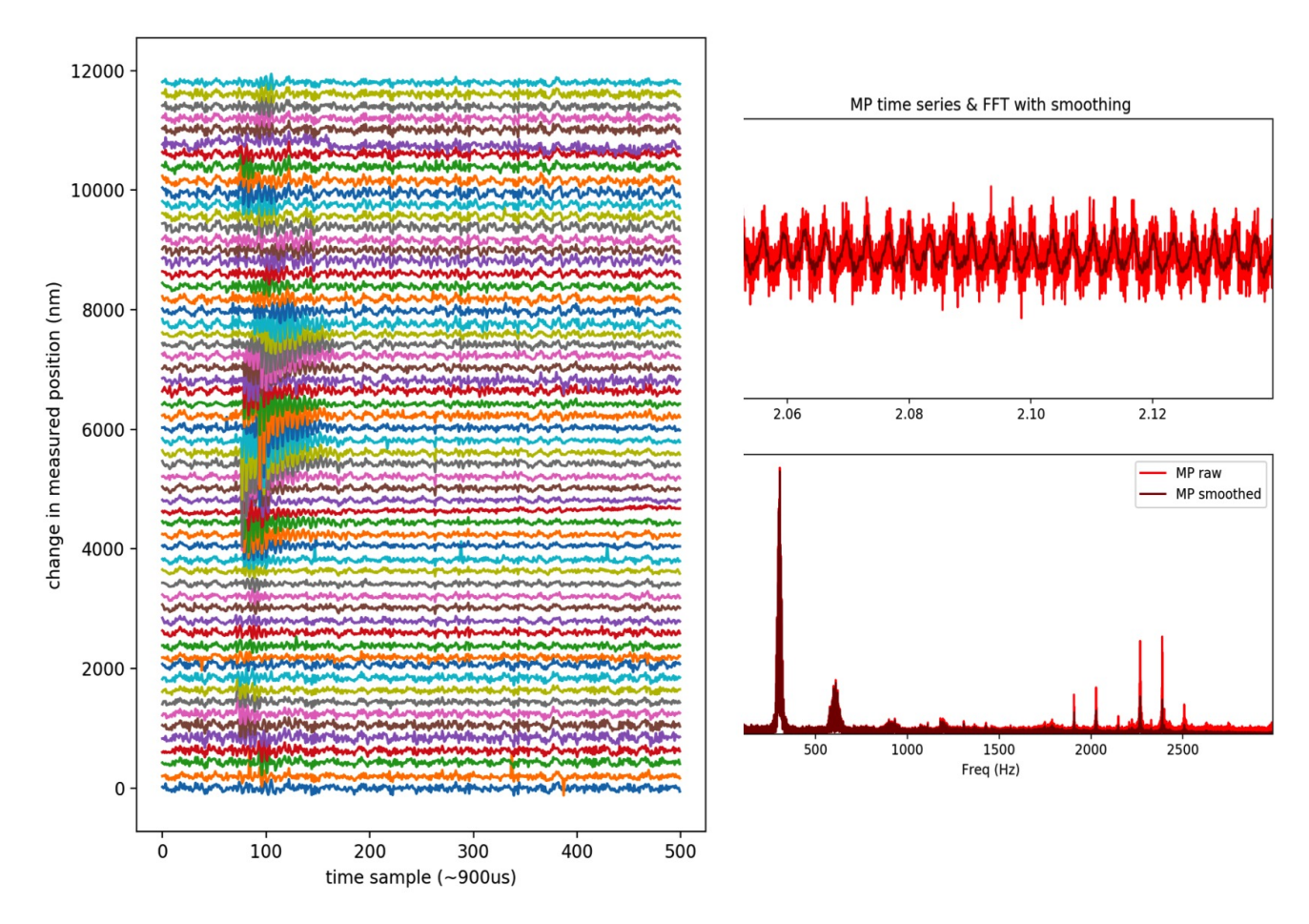


Figure 5 Actuators checkout: Two particular varieties of measurement noise seen at the actuator level. **Left**: in testing mode, we send a periodic command that requests all reportable values from all actuators. In doing so, it seems to impart an impulse to all actuators. Seen here is a finely-sampled time series of multiple actuators, taken across one of those impulses, and the very characteristic "ringing" that results. Actuators are offset along the vertical axis for clarity of plotting. **Right**: a more constant periodic variation in measured position of a single actuator, and its FFT. We see several sharp, distinct, and everpresent frequency peaks in actuator measured positions. Damping and bracing of the mirror stand has lessened them since this particular data was obtained.

Note that this calibration is only an "electrical" one: it adjusts the mathematical relationship between capacitive sensor measurement and reported position gap, but the position gap itself may not correspond with reality.

4. ELECTRICAL AND OPTICAL TESTING

4.1 PID Loop Tuning

In order to maintain a certain gap at each actuator, we need to tune the parameters of the closed-loop actuator control law. We obtain a rough tuning of the Proportional (K_p) and Integral (K_i) gains by increasing K_p until the realtime-reported 1-s rms of MeasuredPosition has approximately doubled, then reducing that value by a factor of 4. Figures 10–11 illustrate this in more detail.

Because most of the tests and calibrations to this point are more sensitive to interruptions than to speed — i.e., we can easily wait for things to settle, but a safety-stop is too disruptive — we've generally used a very

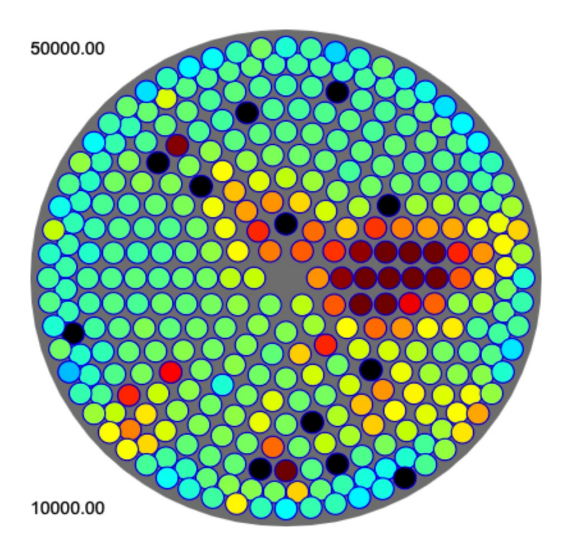


Figure 6 Plotted here: MeasuredPosition values after trying to load a flat with an unclean gap. The pool of lava at 3:00 was the work of a single small metallic crumb of 40 μ m. Yellow regions at 4:30 and 7:30 may also harbor physical particles, but were within an acceptable threshold. Contaminants inside the gap required the shell to be removed, cleaned, and then re-mounted.

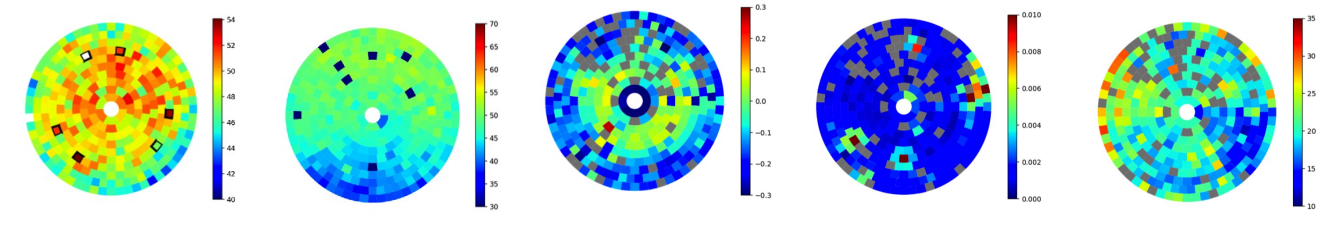


Figure 7 From left to right: 1: Actuator temperature map, with hexapod actuators outlined in black. 2: Same shell, an hour later, after directing a small fan at the 6:00 edge. 3: Force applied by each actuator to maintain a "relaxed flat". 4: Time jitter rms of measured coil currents while holding a flat. Red spots match up to known delinquents. 5: Time jitter rms or measured position (capacitive sensor) while holding a flat. Wedge shapes suggest some daughterboard dependent factor.



Figure 8 Armature inspection. Left to right: complete ring, edge ring, worst-scraped ring.

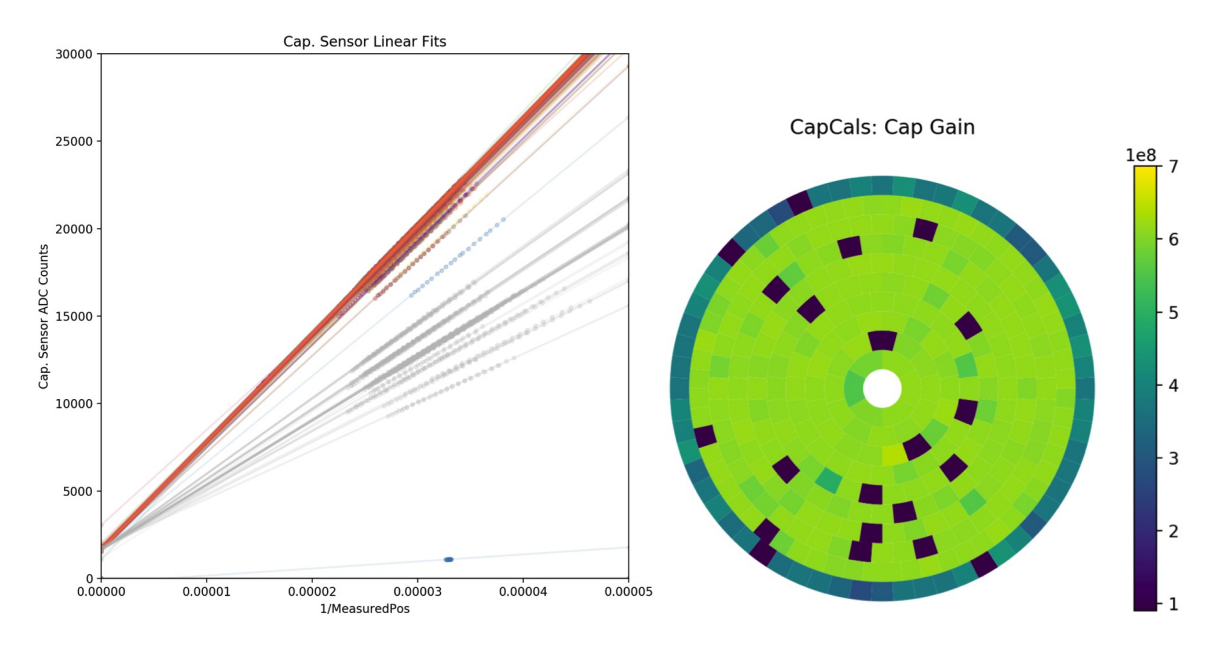


Figure 9 We check the model and refine the calibration by measuring ADC counts and reported position for a range of achievable gaps (here approximately 30000 to 40000 nm). The resulting values for the Gain parameter retain the notable difference between edge actuators and their fully-circled fellows.

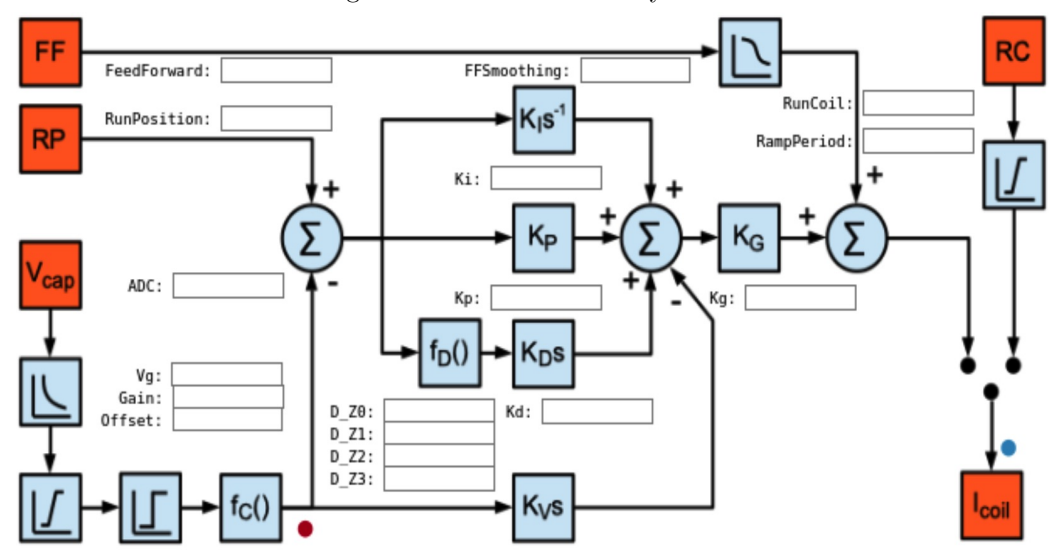


Figure 10 Diagram of the inner loop control scheme.

conservative set of parameters: for a gap of 35 μ m, a reliable but conservative tuning is given with parameters of $K_p = 400$, $K_i = 0.05$.

4.2 Feed-Forward Matrix Measurement

We ensure that the mirror response is fast enough for on-sky operation by using a parallel feed-forward path in the control law. The feed-forward matrix provides a "best guess" for the set of coil currents necessary to achieve a given set of measured gap positions.

A calibrated feed-forward is critical to achieving sub-1ms settling times, especially for modes of higher spatial frequency. In its most basic form, a FF matrix can be determined by applying a known delta-position and

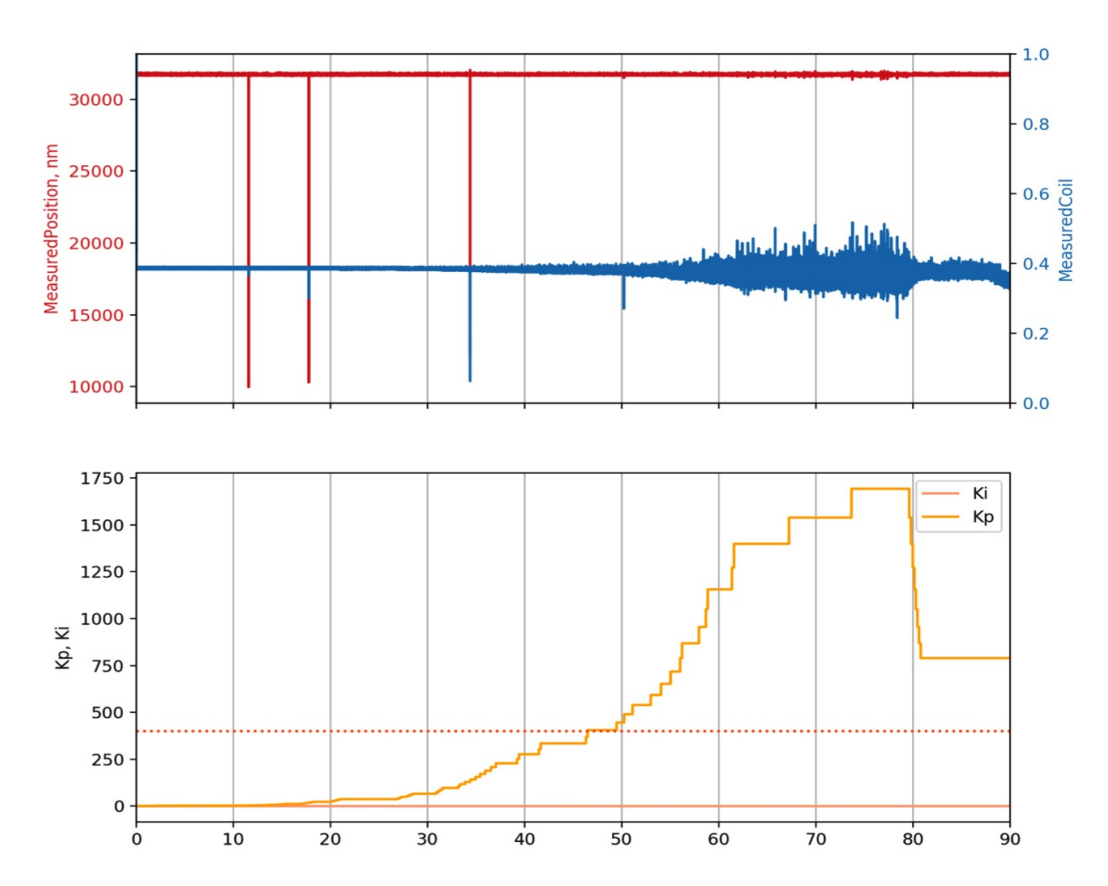


Figure 11 A representative tuning run.

measuring the coil current across all actuators. We command a single modal displacement, applied with ONLY proportional gain in a plus-minus square wave. From there we can derive the actuator-actuatos matrix, whose pattern is, in essence, the answer to "what currents do I need on ALL actuators in order to have a measurable movement on only ONE?" Figure 12 shows the feed-forward matrix measurement.

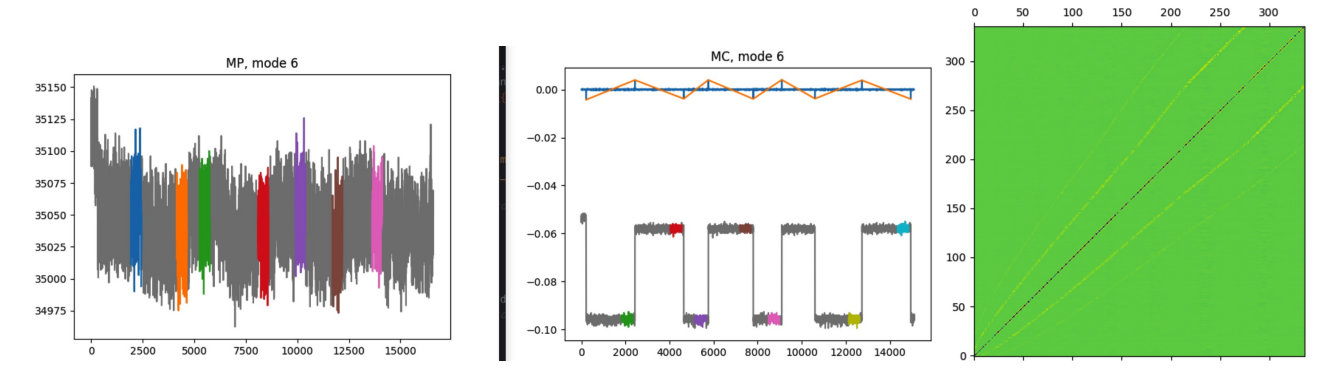


Figure 12 Feed-forward matrix measurement.

4.3 Electrical Results

With even the rudimentary first-pass loop gains and FF matrix we have acquired so far, we are able to command and hold Zernike modal shapes through at least mode 200, and with mirror surface amplitudes of up to 300 nm.

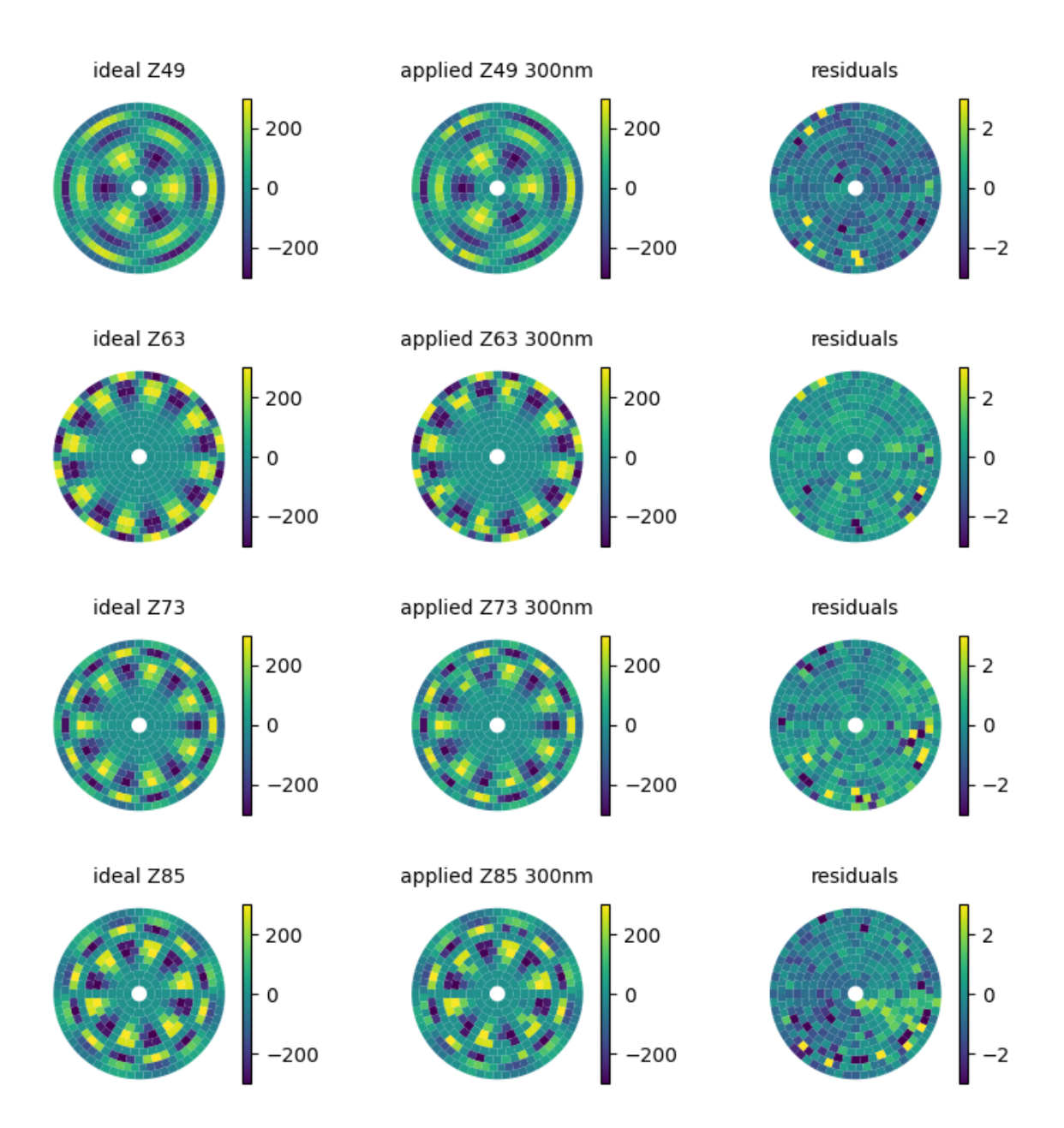


Figure 13 Ideal, applied, and residuals for Zernike modes 49, 63, 73, and 85 of push-pull amplitude 300 nm.

Figures 13–14 show the application of Zernikes to the ASM.

Single-actuator settling times, defined as the time between receipt of the command and the actuator reaching a position that remains within $\pm 10\%$ of nominal, are already <1 ms and, for some actuators, as low as 0.5 ms. Figure 15 shows an example.

Having completed a round of electrical calibration, our next step is to set up a test stand with a light source and interferometer in order to obtain optical measurements.

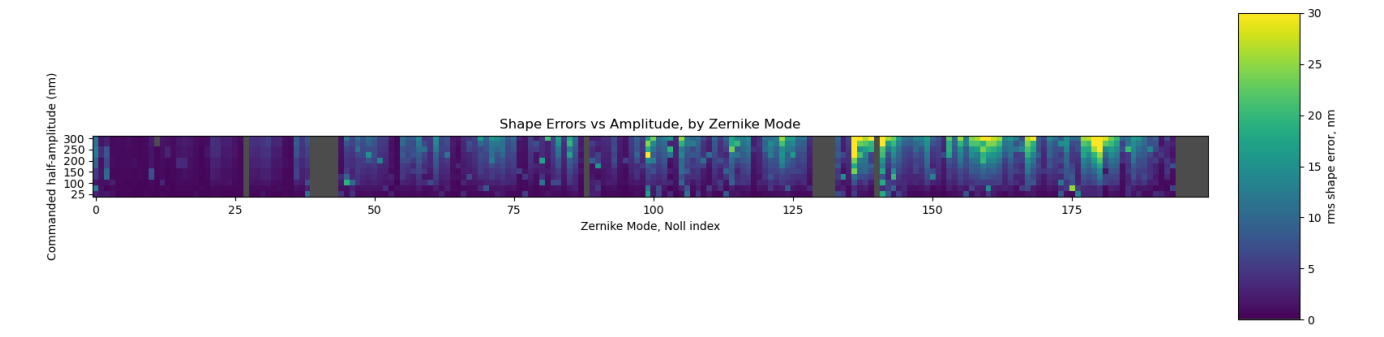
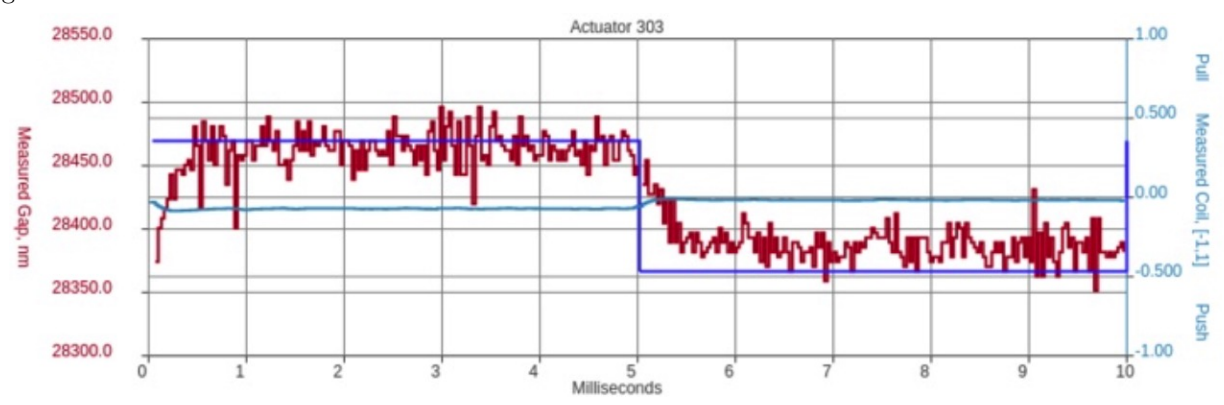


Figure 14 Stroke as a function of Zernike mode.



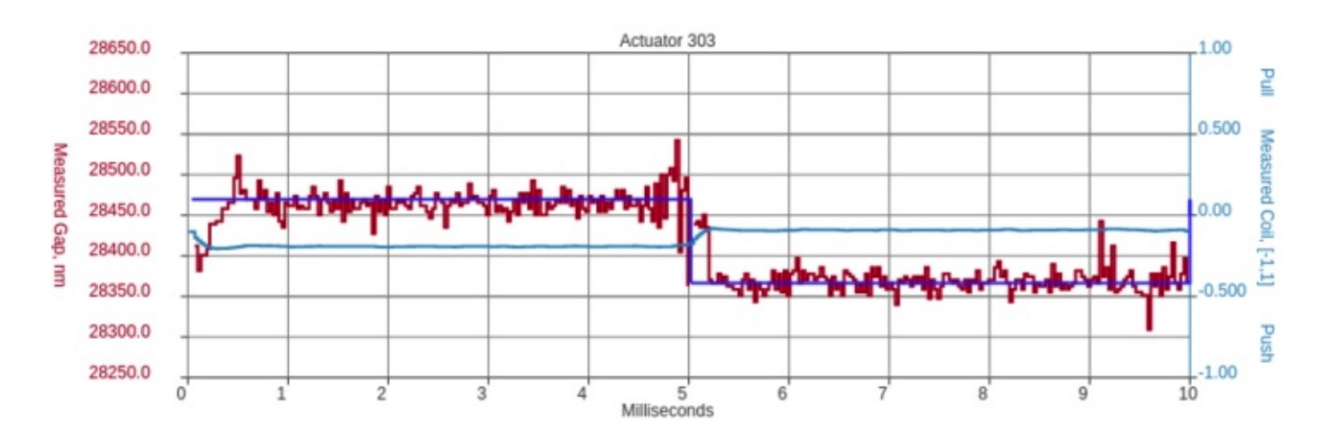


Figure 15 Single-actuator settling time.

5. CONCLUSIONS

We have upgraded, refurbished, and reassembled the MMT ASM in the lab. All of its component systems – computer control, motherboard, daughterboards, actuators, thin shell, and air gap – have passed basic functionality tests. We have confirmed that the fully operational system dissipates approximately 300W of power total, which is sufficiently low to be air-cooled even in our enclosed cleanroom tent.

We have applied Zernike modes 2-200 to the thin shell and verified that the positions reported by the capacitive sensors are, for surface amplitudes up to 300nm, are always within 30nm rms of the target – in fact, with the

exception of a handful of the higher order modes, the surface error is within 10nm rms. This level of spatial performance satisfies the ultimate science requirements of the ASM.

We have made a first calibration of a feed-forward matrix, which will allow us to achieve a settling time of <1ms over the entire shell. So far we have only measured single-actuator settling time, but even with a very rough feed-forward calibration, a single actuator can respond to a step function displacement command of 100nm within 1ms. We thus satisfy the basic temporal performance requirements of the ASM as well.

Our next steps include optical measurement of the surfaces produced, rather than relying entirely on electrical measurements which are subject to errors in calibration. The full calibration process is an iterative one, and we expect that we will use the pending optical measurements to refine a subsequent set of electrical ones, and so on. The results we have obtained with only electrical measurements, though, are encouraging in that they easily meet the performance thresholds. We have already set up an optical test stand and interferometer to measure what will, in the end, be the final desired product of our ASM: an optical wavefront reflecting our every wish.

ACKNOWLEDGMENTS

The MAPS project is primarily funded through the NSF Mid-Scale Innovations Program, programs AST-1636647 and AST-1836008. This research has made use of NASA's Astrophysics Data System. The University of Arizona sits on the original homelands of Indigenous Peoples who have stewarded this Land since time immemorial. Aligning with the university's core value of a diverse and inclusive community, it is an institutional responsibility to recognize and acknowledge the People, culture, and history that make up the Wildcat community. At the institutional level, it is important to be proactive in broadening awareness throughout campus to ensure our students feel represented and valued.

References

- [1] Morzinski, K. M., Montoya, M., Fellows, C., Durney, O., Ford, J., West, G., Gardner, A., Vaz, A., Anugu, N., Mailhot, E., Carlson, J., Harrison, L., Gacon, F., Downey, E., Jones, T., Hinz, P., Patience, J., Sivanandam, S., Chen, S., Lamb, M., Butko, A., Liu, S., Hardy, T., and Jannuzi, B., "Development and status of MAPS, the MMT AO exoPlanet characterization system," in [This Proceedings], Society of Photo-Optical Instrumentation Engineers (SPIE) Conference Series 11448, 11448–61 (2020).
- [2] Anugu, N., Durney, O., Morzinski, K. M., Hinz, P., Sivanandam, S., Males, J., Gardner, A., Fellows, C., Montoya, M., West, G., Vaz, A., Mailhot, E., Carlson, J., Chen, S., Lamb, M., Butko, A., Downey, E., Tyler, J., and Jannuzi, B., "Design and development of a high-speed visible pyramid wavefront sensor for the MMT AO system," in [This Proceedings], Society of Photo-Optical Instrumentation Engineers (SPIE) Conference Series 11448, 11448–332 (2020).